M&C 2017 - International Conference on Mathematics & Computational Methods Applied to Nuclear Science & Engineering, Jeju, Korea, April 16-20, 2017, on USB (2017)

HTR-10 Multiphysics Point Kinetics Benchmark

B. Ganapol, University of Arizona, Tucson, AZ, Ganapol@cowboy.ame.arizona.edu
and
M. DeHart, F. Gleicher, J. Ortensi, S. Schunert and R. Martineau
Idaho National Laboratory, Idaho Falls, ID

Abstract – *A high precision multiphysics point kinetics benchmark is presented to verify the point kinetics solvers in the Rattlesnake transport/diffusion code underdevelopment at INL. Heat transfer from the fuel kernels to the graphite binder within the pebbles and from the graphite pebble to the coolant is included along with the associated reactivity feedback. Both Taylor series and backward Euler algorithms provide highly precise solutions to which the solution from solvers in Rattlesnake will be compared.*

I. INTRODUCTION

We are all very aware of the importance of verification and validation (V&V) for multiphysics applications in nuclear engineering [1]; however, the lack of available high quality multiphysics benchmarks severely limits meaningful V&V. In their absence, we must be satisfied with unit testing, which is generally inconclusive when simulating physical phenomena coupled at a variety of time scales.

What we present here is the first installment of a semi-analytical benchmark to be included in the Multiphysics Test Harness (MTH) for verification of the point kinetics option in the Rattlesnake transport/diffusion code. The class of benchmarks, called semi-analytical, represent highly precise numerical solution evaluations, either directly, or by convergence acceleration of a numerical algorithm. Usually the most precise semi-analytical benchmarks come from evaluations in closed form. Unfortunately, closed form multi physics solutions are virtually non-existent and one must therefore contend with solutions formulated from infinite series, finite difference or elements and/or Picard iteration. Recently, with the emergence of convergence acceleration, one can accelerate solutions based on discretizations or Taylor series to the true solution as the limit. While not always guaranteed to converge to the correct result, more often than not, they indeed do. In this way, a highly precise solution is obtained simply by rearranging iterates toward a limit in a systematic way to capture the asymptotic behavior of a sequence of numerical solutions toward their limit.

For the multiphysics benchmark to be reported, we consider the HTR-10 PBM reactor [2,3], which was one of the first of its kind. The reactor achieved full power in Tsinghua China in 2003. The core is doubly heterogeneous, where the fuel pebble, roughly the size of a billiard-ball, contains fuel kernels, which themselves contain the fuel encased in pyrolytic carbon and silicon carbide coatings as shown in Fig. 1. The graphite matrix of the pebble serves as the moderator as well as the kernel binder. The pebbles then fill a cylindrical core and each slowly moves downward through the core to eventually drop out the bottom as another enters the top. Table I gives the primary HTR-10 reactor design parameters.

The multiphysics model to simulate the initial critical experiment [3,4] includes transient power variation from Doppler feedback from both fuel and moderator. The first solution to the coupled set of dynamic equations comes from a Taylor series representation of the solution analogous to the **CATS** algorithm [5].

Table I. 10MW Reactor primary design parameters [2]

Initial power	$N(0)$	10MW
Initial fuel temperature	$T_F(0)$	853°C*
Initial moderator temperature	$T_M(0)$	827.6°C
Constant coolant temperature	T_∞	748°C
Kernel radius	r	0.00025m
Pebble radius	R	0.03m
Fuel kernels/pebble	n_{fp}	8335
Avg. fuel specific heat	C_{pF}	316.1063 J/kg°K
Avg. moderator specific heat	C_{pM}	1855.9 J/kg°K
Fuel/Moderator heat transfer coefficient**	h	657.7343 W/°Km^2
Number of pebbles	N_p	16888
Fuel to dummy pebble ratio	ξ	0.57
Fuel density	ρ_F	10400 kg/m^3
Moderator density	ρ_M	1730 kg/m3

* All temperatures are in °C

**It appears that in Ref. 3, the temperature used to specify h is incorrectly taken as 748°K rather than 748°C.

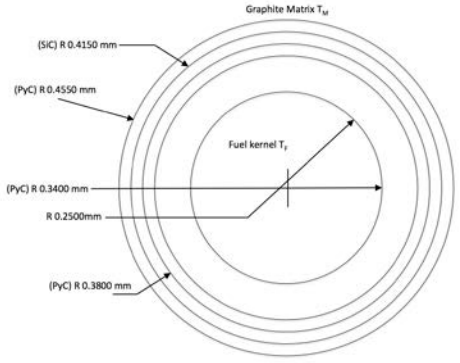

Fig. 1 Fuel particle.

II. THE REACTOR KINETICS/HEAT TRANSFER MODEL

The reactor kinetics model begins with the point kinetics equations (PKEs) for the power and precursor concentrations $N(t)$ and $C_l(t)$

$$\frac{dN(t)}{dt}=\left[\frac{\rho(t,T_F,T_M)-\beta}{\Lambda}\right]N(t)+\sum_{l=1}^{m}\lambda_l C_l(t)+q(t)$$
$$\frac{dC_l(t)}{dt}=\frac{\beta_l}{\Lambda}N(t)-\lambda_l C_l(t),\ \ l=1,...,m, \qquad (1a,b)$$

for *m* delayed neutron groups, which will be either one or six. The initial steady state power is $N(0)$ to give the initial precursor concentrations

$$C_l(0)=\frac{\beta_l}{\lambda_l\Lambda}N(0),\ \ l=1,...,m. \qquad (1c)$$

$\rho(t,T_F,T_M)$ is the reactivity, depending upon both fuel and moderator temperatures. All other symbols have their usual meaning

Λ	Neutron generation time
β_l	Delayed neutron yield for group *l*
β	$\sum_{l=1}^{m}\beta_l$
λ_l	Delayed group decay constant.

We assume Doppler feedback reactivity from both the fuel and moderator in the form

$$\rho(t,T_F,T_M)=\rho_0(t)+\alpha_F\left[T_F-T_F(0)\right]+ +\alpha_M\left[T_M-T_M(0)\right] \qquad (1d)$$

where α_F and α_M are known temperature reactivity coefficients. Table II provides the reactor kinetics parameters for our investigation.

Table II. Precursor yields and decay constants

l	β_l	λ_l(*s*)
1	0.000285	0.0127
2	0.0015975	0.0317
3	0.001410	0.115
4	0.0030525	0.311
5	0.00096	1.40
6	0.000195	3.87

Total yield	β	0.0075
Neutron life time	Λ	0.00168*s*
Fuel reactivity coefficient [2]	α_F	$-1.9\cdot10^{-5}$/°K
Moderator reactivity coefficient [2]	α_M	$-15.7\cdot10^{-5}$/°K

The fuel and moderator temperatures obey the following heat balance equations for constant specific heats:

–– between the fuel and moderator

$$m_F C_{pF}\frac{dT_F(t)}{dt}=N(t)-U\left[T_F(t)-T_M(t)\right] \qquad (2)$$

––between the moderator and flowing helium coolant

$$m_M C_{pM}\frac{dT_M(t)}{dt}=U\left[T_F(t)-T_M(t)\right]-hA\left[T_M(t)-T_\infty\right] \qquad (3)$$

respectively. The total contact area between all pebbles and coolant is

$$A=4\pi R^2 N_p, \qquad (4a)$$

where N_p is the total number of pebbles. The fuel and moderator masses are

$$m_F=\frac{4}{3}\pi r^3\rho_F n_{pf}N_p\xi,\ m_M=\frac{4}{3}\pi R^3 N_p\rho_M. \qquad (4b,c)$$

The only properties left to determine are *U* and *hA* for the given initial power *N*(0) and temperatures $T_F(0),T_M(0)$ and the number of pebbles. One most easily finds these by noting that transient initiation occurs at thermal equilibrium to give, in terms of the initial power and temperatures,

$$U=\frac{N(0)}{\left[T_F(0)-T_M(0)\right]},\ \ hA=\frac{N(0)}{\left[T_M(0)-T_\infty\right]}. \qquad (5a,b)$$

Finally, given *h*, one finds the total number of pebbles, N_p using Eq(4a) since

$$hA=\frac{N(0)}{\left[T_M(0)-T_\infty\right]}=4\pi R^2 N_p h$$

to give

$$N_p=\frac{N(0)}{4\pi R^2 h\left[T_M(0)-T_\infty\right]} \qquad (6)$$

which we round to the nearest integer.

We are now ready to describe the first solution algorithm, called **HTRCATS**.

1. Taylor Series (TS) Formulation

We recast the model equations as a vector ODE in the time interval $t_{j-1}\le t\le t_j$

$$\frac{d\boldsymbol{y}_j(t)}{dt} = \boldsymbol{A}_j\left(t, T_F, T_M\right)\boldsymbol{y}_j(t) + \boldsymbol{q}_j(t), \tag{7a}$$

with

$$\boldsymbol{y}_j(t) \equiv \left[N_j(t) \;\; C_{1j}(t) \;\; .... \;\; C_{mj}(t) \;\; T_{Fj}(t) \;\; T_{Mj}(t) \right]^T$$

$$\boldsymbol{q}_j(t) \equiv \left[0 \;\; 0 \;\; .... \;\; 0 \;\; \frac{hA}{m_M C_{pM}} T_\infty \right]^T. \tag{7b,c}$$

The Jacobian, $\boldsymbol{A}_j$, of size m+3, is

$$\boldsymbol{A}_j(t, T_F, T_M) \equiv$$

$$\equiv \begin{bmatrix} \left(\rho\left(t, T_{Fj}, T_{Mj}\right) - \beta\right)/\Lambda & \lambda_1 & .... & \lambda_m & 0 & 0 \\ \beta_1/\Lambda & -\lambda_1 & 0 & .... & .... & 0 \\ ... & & ... & & & .... \\ \beta_m/\Lambda & .... & & -\lambda_m & & 0 \\ 1/m_F C_{pF} & 0 & .... & 0 & -U/m_F C_{pF} & U/m_F C_{pF} \\ 0 & 0 & .... & 0 & U/m_M C_{pM} & -(U+hA)/m_M C_{pM} \end{bmatrix} \tag{7d}$$

and the initial condition vector is

$$\boldsymbol{y}(0) = \left[N(0) \;\; \frac{\beta_1}{\lambda_1 \Lambda} N(0) \;\; .... \;\; \frac{\beta_m}{\lambda_m \Lambda} N(0) \;\; T_F(0) \;\; T_M(0) \right]^T. \tag{7e}$$

The proposed solution is the following (vector) Taylor series in the time interval $t_{j-1} \le t \le t_j$:

$$\boldsymbol{y}_j(t) = \sum_{n=0}^{\infty} \boldsymbol{y}_{n,j-1} \left(t - t_{j-1}\right)^n. \tag{8a}$$

If, in addition, one expresses the Jacobian matrix as its matrix Taylor series

$$\boldsymbol{A}_j\left(t, T_F, T_M\right) = \sum_{n=0}^{\infty} \boldsymbol{a}_{n,j-1} \left(t - t_{j-1}\right)^n, \tag{8b}$$

and notes

$$\boldsymbol{A}_j\left(t, T_F, T_M\right) \boldsymbol{y}_j(t) = \sum_{n=0}^{\infty} \sum_{l=0}^{n} \boldsymbol{a}_{n-l,j-1} \boldsymbol{y}_{l,j-1} \left(t - t_{j-1}\right)^n,$$

when we introduce all Taylor series into the PKEs, the following recurrence for the power coefficients results for $n \ge 1$:

$$N_{n,j} = \frac{1}{n} \left\{ \begin{array}{l} \dfrac{1}{\Lambda} \left[\begin{array}{l} \left\{ \rho_0 - \beta + \left(\alpha_F \left[T_{F0,j} - T_F(0) \right] + \alpha_M \left[T_{M0,j} - T_M(0) \right] \right) \right\} N_{n-1,j} + \\ + \sum_{l=0}^{n-2} \left(\alpha_F T_{Fn-1-l,j} + \alpha_M T_{Mn-1-l,j} \right) N_{l,j} \end{array} \right] + \\ + \sum_{m=1}^{M} \lambda_m C_{m,n-1.j} \end{array} \right\} \tag{9a}$$

and for precursors and temperatures

$$C_{l,n,j} = \frac{1}{n} \left\{ \frac{\beta_l}{\Lambda} N_{n-1,j} - \lambda_l C_{l,n-1,j} \right\}, l = 1, ..., m \tag{9b}$$

$$T_{F,n,j} = \frac{1}{m_F C_{PF}} \frac{1}{n} \left\{ N_{n-1,j} - U\left[T_{F,n-1,j} - T_{M,n-1,j} \right] \right\}$$

$$T_{M,n,j} = \frac{1}{m_F C_{PF}} \frac{1}{n} \left\{ \begin{array}{l} U\left[T_{F,n-1,j} - T_{M,n-1,j} \right] - hAT_{M,n-1,j} + \\ + hAT_\infty \delta_{n-1} \end{array} \right\}. \tag{9c,d}$$

2. Limit of Taylor Series

Thus, from the initial conditions (j = 0), we find all subsequent Taylor series coefficients and the solution is analytical, but not in closed form, however analytical nevertheless. Therefore, the true analytical solution is the limit

$$\boldsymbol{y}_j(t) = \lim_{N \to \infty} \sum_{n=0}^{N} \boldsymbol{y}_{n,j-1} \left(t - t_{j-1}\right)^n. \tag{10}$$

Using the concept of convergence acceleration in the form of the Wynn-epsilon (*W-e*) extrapolation [6], one can realize the limit to high precision. This we accomplish by considering the limit as a sequence of solutions and rearranging the sequence using *W-e* acceleration to capture the asymptotic approach to the limit more rapidly than the original sequence. Richardson acceleration [6] also enters into the overall evaluation.

III. NUMERICAL IMPLEMENTATION AND VERIFICATION: CONSTANT SPECIFIC HEAT CAPACITIES

1. Numerical Implementation

Numerical implementation begins with the input including the desired edits t_e by defining intervals $[t_{e-1}, t_e]$. Since each edit interval is treated sequentially in time, each is independent and is to be converged relative to a sub-grid within the interval as now described. We begin with the first interval between time zero and the first edit $[0, t_1]$. One constructs the interval sub-grid by continually halving the original interval. In this way, a sequence of solutions at the interval end point $[t_1(l)]$ is generated based on the sub-discretization ($1/2^l$, l=1,…,12), whose convergence (in l) is accelerated by Richardsons acceleration. If the discretization exceeds 12 subdivisions (2^{12}), the original edit interval $[0, t_1]$ is halved and the process restarts. This continues until 2^{12} subdivisions of the original interval; after which, the program terminates indicating failure to converge. Recall that for all evaluations, a converged Taylor series solution from Eq(8a) is necessary. We require convergence to be within a fixed number of terms with help from the *W-e* algorithm. If unsuccessful, the calculation jumps to the next sub-grid (l+1) of the interval $[0, t_1]$ and continues until convergence of the interval end point

solution or failure as described above. If the interval end point solution has converged in l, we go on to the next interval $[t_1,t_2]$ with a highly converged initial condition reducing the propagation error. We remark that the convergence acceleration just described enables such a high quality benchmark.

2. Initial Demonstration

The four benchmarks we consider are those found in Ref. 3 for step reactivity insertions of ρ_0 = 0.05\$, 0.25\$, 0.50\$ and 1.0\$ assuming constant specific heats and the 10MW design parameters of Table I.

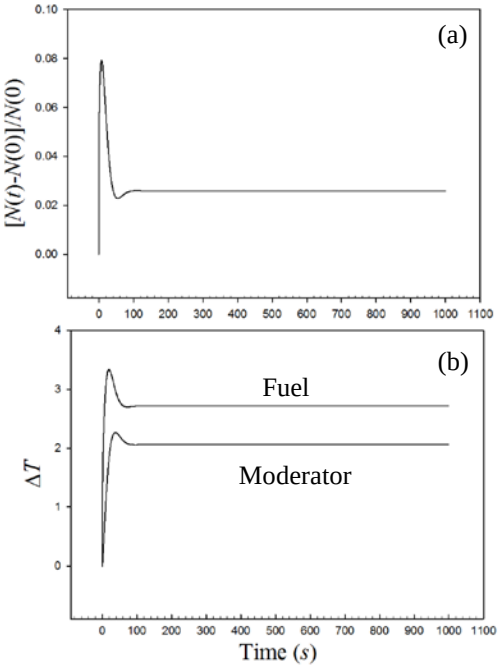

Fig. 2. Reactor response for 0.05\$ reactivity insertion (a) $[N(t)-N(0)]/N(0)$, (b) ΔT_F, ΔT_M.

Figure 2 shows the relatively quiescent response of the HTR-10 reactor for a 0.05\$ step reactivity insertion. Similarly, Fig. 3 shows correspondingly larger power spikes for stronger insertions never exceeding four times $N(0)$.

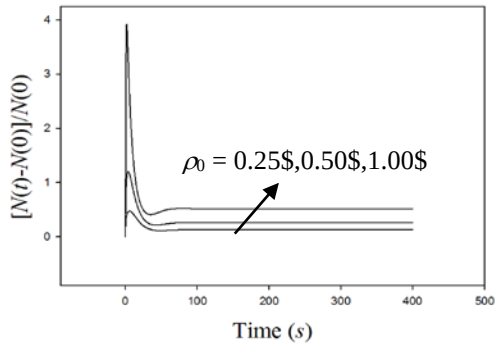

Fig. 3. Reactor power response for reactivity insertions of 0.25, 0.5 and 1\$.

We now observe the difference between one- and six-group delayed neutron models. For an insertion of 0.05\$, the power, fuel and moderator temperature transients are

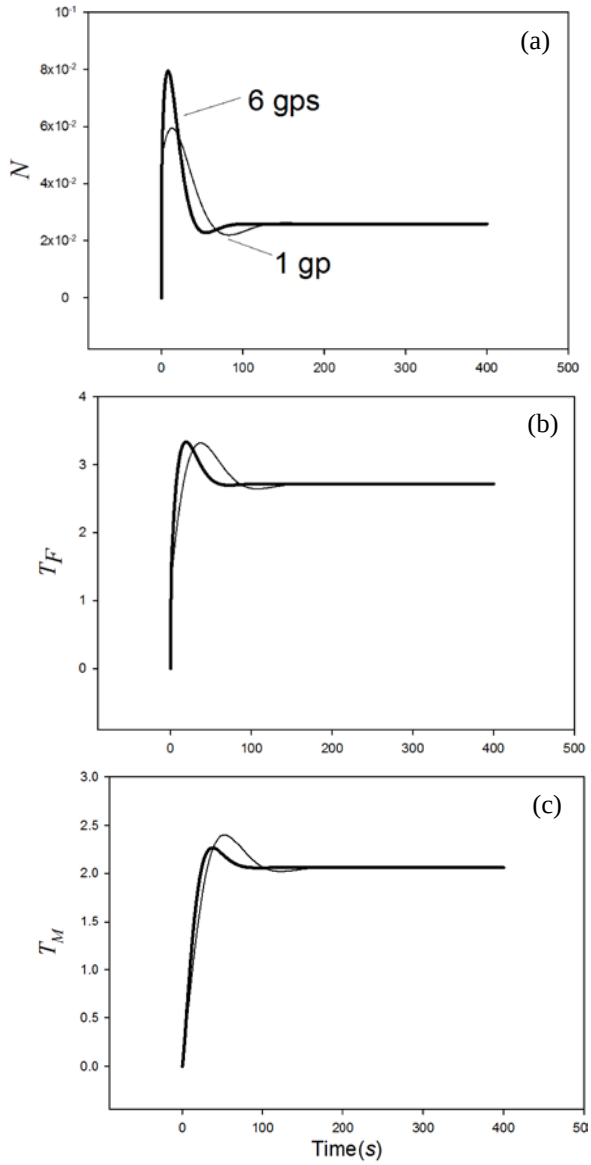

Fig. 4. Comparison of one and six groups of delayed neutrons for (a) Power, (b) Fuel temperature, (c) Moderator temperature for 0.05\$ insertion.

shown in Fig.4 for both one and six delayed neutron groups. For a consistent one delayed group using the kinetic parameters of Table II, we calculate λ as

$$\lambda = \beta / \sum_{l=1}^{6} \frac{\beta_l}{\lambda_l} = 0.0784s$$

since β is known.

It seems the 6-group model gives a higher maximum power and shifted temperatures in time. Apparently, more

neutrons are available after the peak from the one group approximation thus shifting the temperature peaks to higher times. Interestingly however, the asymptotic steady state powers for both cases are theoretically (and numerically) identical. One can show this theoretically since to achieve asymptotic steady state, the reactivity must be zero as time approaches infinity, implying from Eq(1d)

$$0 = \rho_0 + \alpha_F \left[T_{F\infty} - T_F(0) \right] + \alpha_M \left[T_{M\infty} - T_M(0) \right] \cdot \quad (11a)$$

In addition, the derivatives of both T_F and T_M in Eqs(2) and (3) must vanish

$$0 = N_\infty - U \left[T_{F\infty} - T_{M\infty} \right] \quad (11b)$$

$$0 = U \left[T_{F\infty} - T_{M\infty} \right] - hA \left[T_{M\infty} - T_\infty \right]. \quad (11c)$$

This gives three equations, whose solution is

$$T_{F\infty} = -\frac{\alpha_M hAT_\infty + (hA+U)\left(\rho_0 - \alpha_F T_F(0) - \alpha_M T_M(0)\right)}{\alpha_M U + \alpha_F (hA+U)}$$

$$T_{M\infty} = -\frac{-\alpha_F hAT_\infty + U\left(\rho_0 - \alpha_F T_F(0) - \alpha_M T_M(0)\right)}{\alpha_M U + \alpha_F (hA+U)} \quad (12a,b)$$

$$N_\infty = U \left(T_{F\infty} - T_{M\hbar} \right),$$

which depend only the heat transfer parameters and reactivity. Thus, the steady state power is independent of the delayed neutrons as one would expect for steady state.

Table III gives 9-place power and temperatures for benchmark comparison purposes. It should be noted that the

Table III. Benchmark values for 0.05$ insertion from **HTRCATS** for uniform specific heat

t	*N*	T_F	T_M
1.0000E-01	1.018125306E+07	8.532930142E+02	8.276007592E+02
1.0000E+00	1.056325348E+07	8.544755043E+02	8.276630729E+02
1.0000E+01	1.078209325E+07	8.560334558E+02	8.286504435E+02
1.0000E+02	1.025902824E+07	8.557145498E+02	8.296566325E+02
5.0000E+02	1.025875839E+07	8.557169439E+02	8.296596976E+02
1.0000E+03	1.025875988E+07	8.557169787E+02	8.296597286E+02
1.5000E+03	1.025875988E+07	8.557169788E+02	8.296597287E+02

last value in the table corresponds exactly to the theoretical results of Eqs(12).

3. Comparison to Rattlesnake (RS) PKE solvers

Figure 5 shows our first benchmark comparison for 0.05$ insertion with two of the RS/PKE solvers for a time step of 0.05*s* indicating excellent agreement of the power at late times. The BDF-2 multistep solver seems to slightly outperform the single step Implicit Euler solver. Interestingly, the imprecise powers at initial times do not contaminate later powers. Indeed, the asymptotic values are essentially identical to the theoretical values shown in Table IV for coarser step sizes. This is a consequence of the asymptotic values, computed by solving a nonlinear (in general) system of equations, which Rattlesnake solves to iterative tolerance independent of time step size.

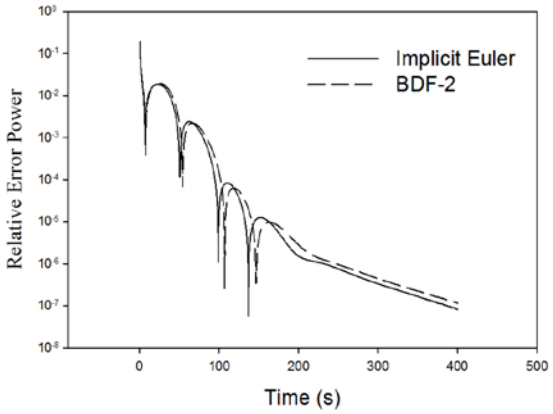

Fig. 5. Comparison or RS solvers to **HTRCATS** results for 0.05$ benchmark.

Table IV. Asymptotic comparison for 0.05$ insertion

	$(N_\infty - N(0))/N(0))$	ΔT_F	ΔT_F
HTRCATS	2.58759882E-02	2.716978724	2.059728625
RS(1s)	2.5875988E-02	2.716978719	2.059728620
RS(0.1s)	2.5875988E-02	2.716978724	2.059728624
RS(0.5s)	2.5875988E-02	2.716978724	2.059728624

IV. VARIABLE SPECIFIC HEAT CAPACITIES

Of course, in a real simulation of the HTR10, the specific heat capacities of the fuel and moderator will depend strongly on their respective temperatures. Therefore, a proper simulation requires a model of the temperature dependence of the heat capacity of UO_2 and graphite, which one finds to be

–– for UO_2 [8] with T_F in the range [298.15°K, 3120°K]

$$C_{pF}(T_F) = \frac{1000}{267}\left[\begin{array}{l} 52.1743 + 87.951\zeta - 84.2411\zeta^2 + \\ +31.542\zeta^3 - 2.6334\zeta^4 - \dfrac{0.71391}{\zeta^2} \end{array}\right]$$

$$\zeta \equiv \frac{T_F}{1000} \quad (13)$$

–– for graphite [2] with T_M in the range [298°K, 1273°K]

$$C_{pM}(T_M) = 10^3 \left[\begin{array}{l} 1.131 + 6.62x10^{-4} T_M - \\ -9.9691x10^{-8} T_M^2 \end{array}\right]. \quad (14a)$$

and in the range [1273°K, 3273°K]

$$C_{pM}\left(T_M\right)=10^3\begin{bmatrix}2.031+7.8645x10^{-5}T_M^2\\-4.2671x10^5T_M^{-1}+1.3203x10^8T_M^{-3}-\\-1.199x10^{10}T_M^{-4}\end{bmatrix}. \quad (14b)$$

The Jacobian now becomes

$$A\left(t,T_F,T_M\right)\equiv$$

$$\equiv\begin{bmatrix}\left(\rho\left(t,T_F,T_M\right)-\beta\right)/\Lambda & \lambda_1 & .... & \lambda_m & 0 & 0\\ \beta_1/\Lambda & -\lambda_1 & 0 & .... & .... & 0\\ ... & & ... & & & ....\\ \beta_m/\Lambda & .... & & -\lambda_m & & 0\\ 1/m_FC_{pF}\left(T_F\right) & 0 & .... & 0 & -U/m_FC_{pF}\left(T_F\right) & U/m_FC_{pF}\left(T_F\right)\\ 0 & 0 & .... & 0 & U/m_MC_{pM}\left(T_M\right) & -\left(U+hA\right)/m_MC_{pM}\left(T_M\right)\end{bmatrix} \quad (15)$$

with non-linear heat capacities included in the bottom two rows. A Taylor series solution is no longer possible because the heat capacities do not admit Taylor series in general. Hence, we turn to the **BEFD** solution algorithm [7].

The **BEFD** algorithm is one of the simplest solvers of ODEs. It employs the backwards finite difference to implicitly solve Eq(7a) to high order. Essentially, the numerical procedure is the same as for **HTRCATS** with the Taylor series replaced by the **BEFD** algorithm, which solves Eq(7a) including an iteration to accommodate the nonlinear Jacobian. More detail of the numerical implementation is found in Refs. [7] and [9].

We ran the **BEDF** algorithm for the 0.05$ transient with constant specific heats and found the identical values in Table III. Such a comparison is a necessary verification of the **BEDF** algorithm.

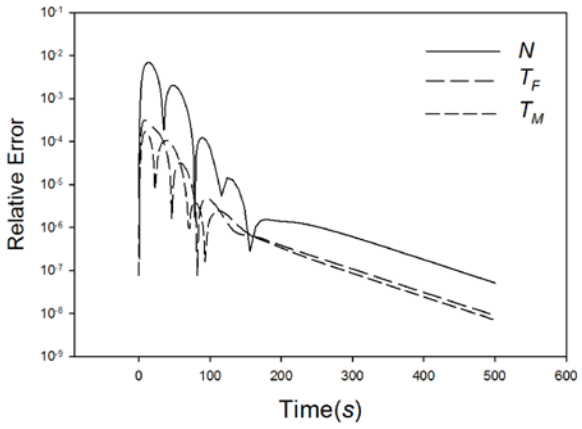

Fig. 6. Variation of power with and without uniform specific heats for 1$ insertion.

Figure 6 shows the relative error with and without variation of the specific heats for a 1$ insertion. For this strong transient the largest relative error is less than 1% for power and even less for temperatures These low relative errors confirm using constant specific heats is a reasonable assumption, also a conclusion of Ref. [3]. Eventually, we will the **RS/PKE** solvers to the HTR-10 PBMR with temperature dependent specific heats.

V. PRELIMINARY CONCLUSION

It is clear that several high quality multiphysics benchmarks have been established for the HTR-10 PBMR. These are a Taylor series solution (**HTRCATS**) for constant specific heats and a backward Euler finite difference (**BEFD**) for variable specific heats. A first test of two of the Rattlesnake solvers has shown excellent agreement at late times in the transient. The discrepancy at earlier time is under investigation. The next step in the benchmarking of the Rattlesnake code will be to run Rattlesnake's additional solvers for a variety of time steps to enable a meaningful qualitative assessment of all the ODE solvers in the **RS/PKE** option.

NOTE IN CLOSING

The results included in this work are based on the moderator mass computed by Eq. (4c). Ref. [3] presents results that are in marked visual disagreement with ours– for both **HTRCATS** and **RS/PKE**, which were generated independently by two authors of this paper. Trial and error showed that we can reproduce Ref. [3]'s results with a moderator mass three times as large as the one computed using Eq. (4c). Therefore, we suggest that there might an error in the computation of the moderator mass used in Ref. [3].

REFERENCES

1. O. Zerkak, T. Kzlowski and I. Gajev, Review of multi-physics temporal coupling methods for analysis of nuclear Reactors, *Annals of Nuclear Energy*, 85, pp. 225-233 (2015).
2. Z. Wu, D. Lin, D. Zhong, The design features of the HTR-10, *Nuclear Engineering and Design*, 218 pp. 25–32, 2002.
3. S. Hosseini, Dynamic Behavior of the HTR-10 Reactor: Dual Temperature Feedback Model, NT&RT, VXXX, No. 2, pp 83-163. 2015.
4. William K. Terry, et.al., Evaluation of the HTR-10 Reactor as a Benchmark for Physics Code QA, PHYSOR-2006, ANS Topical Meeting on Reactor Physics, 2006.
5. B. Ganapol, et. al, The Solution of the Point Kinetics Equations via Converged Accelerated Taylor Series (**CATS**), PHYSOR 2012, Knoxville, TN, ANS M&C Topical Meeting on Reactor Physics, 2012.
6. A. Sidi, *Practical Extrapolations Methods*, Cambridge University Press, Cambridge, 2003.
7. B. Ganapol, A Highly Accurate Algorithm for the Solution of the Point Kinetics Equations, *Annals of Nuclear Energy*, V62, pp 564-571, 2013.

8. J.K. Fink, Thermophysical Properties of Uranium Dioxide, Journal of Nuclear Materials 279 pp.1-18, 2000.
9. B. Ganapol, et.al., SKINATH Multiphysics Point Kinetics Benchmark, Interim Progress Report, INL, Su2016.